· Article · Advances in Polar Science
doi: 10.13679/j.advps.2018.3.00003 September 2018 Vol. 29 No. 3: 3-19

Simulated impact of Southern Hemisphere westerlies on Antarctic Shelf Bottom Water temperature

LIN Xia[1,2*] & WANG Zhaomin[1,2]

[1] College of Oceanography, Hohai University, Nanjing 210098, China;
[2] International Polar Environment Research Laboratory, Hohai University, Nanjing 210098, China

Received 1 May 2018; accepted 19 September 2018

Abstract The Southern Hemisphere (SH) westerly winds have intensified and shifted poleward since the 1970s and this trend is projected to sustain under future anthropogenic forcing. The influences of intensified SH westerlies on the Antarctic coastal waters are still not clear. The variability of Antarctic Continental Shelf Bottom Water (ASBW) temperature is crucial for ice shelf basal melting and hence ice shelf mass balance in Antarctica. In order to understand the impacts of SH westerlies on the variability of ASBW temperature, atmospheric forcing in 1992 with weak westerlies and in 1998 with strong westerlies are used to drive a high-resolution ocean-sea ice general circulation model, MITgcm-ECCO2. Our simulated results show that under the atmospheric forcing in 1998, the ASBW becomes warmer in most regions around Antarctica except the coastal region between 60°–150°W, than for the case under atmospheric forcing in 1992. The warming of ASBW around Antarctica is due to the intense shoaling and warming of CDW induced by enhanced Ekman pumping as well as strengthened subpolar gyres. The strengthened subpolar gyres favor the transportation of warm water to the coast of Antarctica. The cooling of ASBW along the coast of the western Antarctic Peninsula is caused by stronger coastal currents, which bring colder water downstream from the northwest flank of the Weddell Sea.

Keywords **Southern Hemisphere westerlies, Antarctic Shelf Bottom Water temperature, MITgcm-ECCO2**

Citation: Lin X, Wang Z M. Simulated impact of Southern Hemisphere westerlies on Antarctic Shelf Bottom Water temperature. Adv Polar Sci, 2018, 29(3): xx-xx, doi: 10.13679/j.advps.3.000xx

1 Introduction

The strength of the Southern Hemisphere (SH) westerly winds is found to be closely related to the phase of the Southern Annular Mode (SAM), the dominant atmospheric mode in the SH. The SH westerlies have strengthened and shifted poleward since the 1970s when the SAM index became more positive, and this trend is projected to continue under future anthropogenic forcing (Thompson et al., 2011; Wang et al., 2011; Oke and England, 2004; Marshall, 2003; Thompson and Solomon, 2002; Rind, 1998). Previous model studies investigating the impact of SH westerlies on the temperature of Antarctic coastal waters employed idealized wind forcing by scaling the wind strength with a constant factor and/or by changing the position of the winds by a few degrees in the meridional direction (Fogwill et al., 2014; Spence et al., 2014). Decreased Ekman transport near the coast induced by a poleward wind shift at the latitudes of the Antarctic Peninsula was found to contribute to the warming of subsurface coastal waters (Spence et al., 2014; Gill, 1973). The subpolar gyres induced heat transport variability under a poleward shift of winds during the Last Interglacial and this has been suggested to contribute to subsurface warming around Antarctica (Fogwill et al., 2014). However, the response of coastal water temperature around Antarctica to the recent variability of SH westerlies and the responsible mechanisms are still not clear (Spence et al., 2014).

The Antarctic Continental Shelf Bottom Water (ASBW)

* Corresponding author, E-mail: xiaeergunahe@163.com

overlies the sea floor of the Antarctic continental shelf. It originates from Circumpolar Deep Water (CDW), bottom-reaching Winter Water (WW) or their mixing (Schmidtko et al., 2014). The variability of ASBW temperature is crucial for ice shelf basal melting and hence ice shelf mass balance of Antarctica under continued anthropogenic forcing (Schmidtko et al., 2014; Rignot and Jacobs, 2002). CDW intrusion onto the Antarctic continental shelf can change the ASBW temperature. Both warming and the shoaling of CDW contribute to ASBW warming over the continental shelf of the Bellingshausen and Amundsen seas (Schmidtko et al., 2014). Model studies also indicate the importance of ocean currents in transporting the warm water into the ice shelf cavity, contributing to basal melting (Liu et al., 2017; Webber et al., 2017; Hellmer et al., 2012; Jacobs et al., 2011; Jenkins and Jacobs, 2008). The subpolar and Antarctic continental shelf circulations could also be crucial for the ASBW temperature variability by affecting the heat transport. Therefore, the relationships between SH westerlies, subpolar gyres, CDW intrusion, and ASBW temperature variability around Antarctica needs to be examined.

This paper aims to investigate the response of ASBW temperature variability to the strengthened SH westerlies and to explore the underlying mechanisms. For this purpose, we use realistic atmospheric forcing in different years with different SH westerly wind strength to drive the high-resolution ocean-sea ice model, MITgcm-ECCO2. The paper is structured as follows. The model and the experimental design are described in Section 2. In Section 3, the response of ASBW temperature to the changes in SH westerlies and the underlying mechanisms are analyzed. Finally, a discussion is presented in section 4.

2 Model description and the experiments

The high-resolution ocean-sea ice general circulation model used here is the Estimating the Circulation and Climate of the Ocean, Phase II (ECCO2, Losch et al., 2010; Menemenlis et al., 2008). The configuration of ECCO2 is based on the Massachusetts Institute of Technology general circulation model (MITgcm), which is a three-dimensional coupled ocean-sea ice model based on the Boussinesq approximation and hydrostatic assumption (Marshall et al., 1997a, 1997b). The cube-sphere grid structure with relatively even grid spacing is used to avoid polar singularities (Adcroft et al., 2004). The mean horizontal grid resolution is 18 km with eddy permitting at high latitudes. It has 50 layers in the vertical direction, with intervals ranging from 10 m near the surface to about 450 m at the deepest level of 6135 m. The atmospheric forcing is from the Japanese 25-year Reanalysis dataset (JRA25; Onogi et al., 2007) with six-hourly intervals, including downward short wave and long wave radiation, 10 m surface winds, 2 m air temperature, 2 m humidity and precipitation with a spatial resolution of 1.125°×1.125°. Optimized control parameters are obtained by using the Green function approach to reduce model-data misfit (Menemenlis et al., 2005).

To investigate the response of ASBW temperature to the strengthened SH westerlies, two idealized experiments were designed. Six-hourly atmospheric forcing from weak westerlies in 1992 and from strong westerlies in 1998 is used to drive the model according to the station-based SAM index from Marshall (2003). The model is integrated over 28 years under fixed atmospheric forcing in 1992 and 1998 with an output frequency of 5 days. The model outputs of the last five years (model year 24 to 28) are analyzed in this study.

3 Results

Figure 1 shows the mean zonal wind stress (a–c) and wind stress curl (d–f) under atmospheric forcing in 1992 (a, d), 1998 (b, e) and their differences (c, f) in the Southern Ocean. The mean zonal wind stress under atmospheric forcing in 1998 (Figure 1b) is stronger than that in 1992 (Figure 1a) in the Southern Ocean from around 40°S to 60°S especially in the Pacific section (Figure 1c). The positions of axes of maximum SH zonal wind stress are very close to each other under atmospheric forcing in 1992 and 1998 as shown by the blue (Figure 1a) and black (Figure 1b) lines. The values of the mean wind stress curl under atmospheric forcing in 1998 (Figure 1e) are much smaller than those in 1992 (Figure 1d) in the subpolar ocean, indicating stronger SH cyclonic wind forcing in 1998 in regions such as the Weddell Gyre (WG), Ross Gyre (RG), and the deep Antarctic-Australian Gyre (AG) (Figure 1f).

ASBW is defined as the water mass occupying the sea floor on the Antarctic continental shelf for depths shallower than 1500 m. The temperature of ASBW is defined as the temperature of the water mass just above seabed. Under weak atmospheric forcing in 1992, the ASBW temperature is generally positive around West Antarctica, but negative around East Antarctica (Figure 2a). But under strong atmospheric forcing in 1998, the ASBW temperature becomes positive broadly around Antarctica (Figure 2b). Figure 2c shows warming of ASBW under strong SH westerlies around Antarctica except for the coastal region from 60.125°W to 150.125°W. The cooling of ASBW from 60.125°W to 150.125°W is consistent with a colder ASBW temperatures in the Bellingshausen Sea in 1998 than that in 1992 as found by Schmidtko et al. (2014).

The temperature of CDW, defined as the maximum water mass temperature below 90 m at places where ocean depth exceeds 1500 m, is shown in Figures 2d–2f and the core depth of CDW, defined as the depth of the warmest water mass, is shown in Figures 2g–2i. Broad warming and shoaling of CDW under strong SH westerlies are found in most regions around Antarctica (Figures 2f and 2i), which contribute to the warming of ASBW. The warming and shoaling of CDW is due to increased Ekman pumping under more cyclonic wind stress forcing in 1998 (Figure 1f).

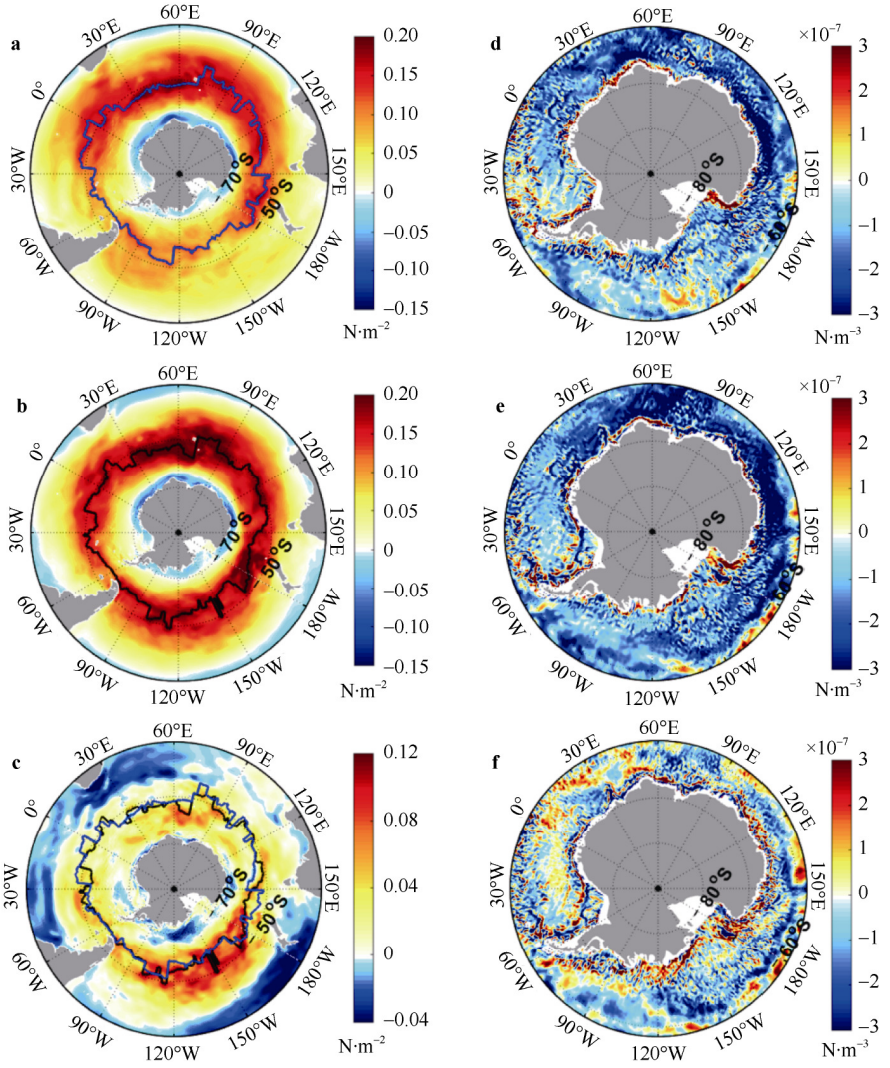

Figure 1 The mean zonal wind stress (N·m^{-2}, **a**–**c**) and wind stress curl (N·m^{-3}, **d**–**f**) under atmospheric forcing in 1992 (**a**, **d**) and 1998 (**b**, **e**). **c** shows **b** minus **a**. **f** shows **e** minus **d**. The axes of the maximum zonal wind stress are marked by blue and black lines in panels **a** to **c**.

Figure 3 shows the speed of ASBW (a–c), barotropic streamfunction (d, e, contour lines), and meridional heat transport of the upper 1007.2 m (d–f, colors) under atmospheric forcing in 1992 (a, d), 1998 (b, e) and their differences (c, f). An increased speed of ASBW under strong SH westerlies is found in many regions around Antarctica, such as from 60.125°W to 150.125°W (Figures 3a–3c). The cooling of ASBW around the coast of the Bellingshausen Sea and Amundsen Sea (Figure 2c) under strong atmospheric forcing in 1998 is caused by the enhanced coastal currents, which bring in much colder water from the northwest of the Weddell Sea.

The WG, RG, and AG are well captured by the simulations, as illustrated by the barotropic streamfunction under different atmospheric forcing (Figures 3d and 3e). Gyre strengths are defined as the maximum barotropic streamfunction values at the gyre centers (Table 1). The three gyres are much stronger under atmospheric forcing in 1998 than in 1992 (Figures 3d vs 3e), which is due to more cyclonic wind forcing in 1998 in the subpolar region (Figures 1f). The strengths of the WG are respectively 62.86 Sv and 70.74 Sv under atmospheric forcing in 1992 and 1998. The measured westward transport of 56±8 Sv across the Prime Meridian, based on 4.5 year-duration moored current measurements (Klatt et al., 2005), is close to the WG strength simulated in our model experiments. The strengths of the RG are respectively 46.04 Sv and 57.10 Sv under atmospheric forcing in 1992 and 1998 in our calculation. Total transport in the subpolar region estimated from hydrographic data across 150°W is 8.5 Sv (Gouretski, 1999), although this is underestimated because it ignores the barotropic component of velocity (Wang and Meredith, 2008; Park and Gambéroni, 1995). The strengths of the AG are respectively 15.28 Sv and 27.28 Sv under atmospheric forcing in 1992 and 1998, which are much lower than the westward flow across 110°E of 76±26 Sv estimated from summer hydrographic data and direct velocity measurements (McCartney and Donohue, 2007). The simulated strengths of the RG and AG are very

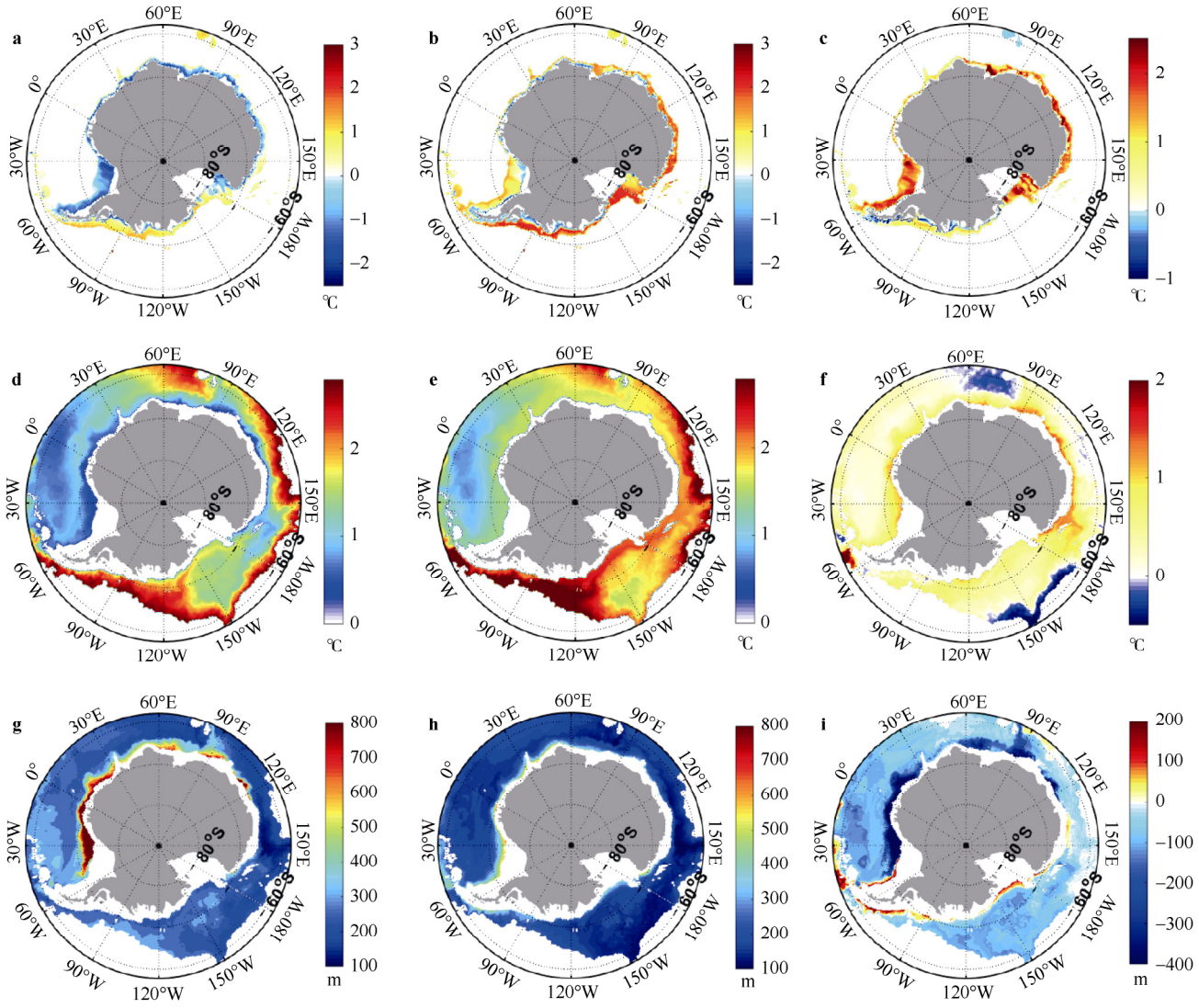

Figure 2 The mean temperature (°C) of ASBW (**a**, **b**) and CDW (**d**, **e**), core depth (m) of CDW (**g**, **h**) under atmospheric forcing in 1992 (**a**, **d**, **g**) and 1998 (**b**, **e**, **h**). **c** shows **b** minus **a**. **f** shows **e** minus **d**. **i** shows **h** minus **g**. The ASBW temperature is the temperature of water mass at the seabed for depths shallower than 1500 m (**a**–**c**). The temperature of CDW is the maximum water mass temperature at the places where ocean depth exceeds 1500 m (**d**–**f**) and the core depth of CDW is the depth of maximum water mass temperature (**g**–**i**). Only regions with the ocean depth exceeds 1500 m and the warm core of CDW is cooler than 2.8°C are shown (**d**–**i**).

different from the observational results, but are comparatively close to the ensemble means of the RG and AG strengths from CMIP5 models of 24±15 Sv and 19±10 Sv, respectively (Wang, 2013). Accurate estimates of gyre strengths are limited in the subpolar ocean due to a lack of long-time observations. More observational data is needed to compare with the simulated strengths of subpolar gyres and to help improve the simulation in the future. We focus on the variability of the gyre strengths under different atmospheric forcing in this study. The gyres are much stronger under atmospheric forcing in 1998 than in 1992 with the differences for WG, RG and AG being 7.88 Sv, 11.06 Sv and 12.00 Sv, respectively (Table 1).

Vertically integrated oceanic meridional heat transport (F) is calculated by the formula

$$F = \rho_0 c_p \int\int v \cdot \theta \mathrm{d}x\mathrm{d}z\,, \quad (1)$$

where ρ_0 is the reference seawater density with $\rho_0 = 1.035 \times 10^3$ kg·m^{-3}, c_p is the specific heat capacity of seawater at constant pressure with $c_p = 4.187 \times 10^3$ J·(kg·℃)$^{-1}$, v is the meridional velocity, θ is the potential temperature, x is the horizontal coordinate and z is the vertical coordinate. Vertically integrated meridional heat transport in the upper 1007.2 m is assessed under atmospheric forcing in 1992 (Figure 3d) and 1998 (Figure 3e). The gyre circulation transports warm water to the Antarctic coast in the eastern branches of the gyres, and cold water is transported away from the Antarctic coast in the western branches of the gyres (Figures 3f). Increased ASBW speed under strong atmospheric forcing in 1998 (Figure 3c) tends to transport

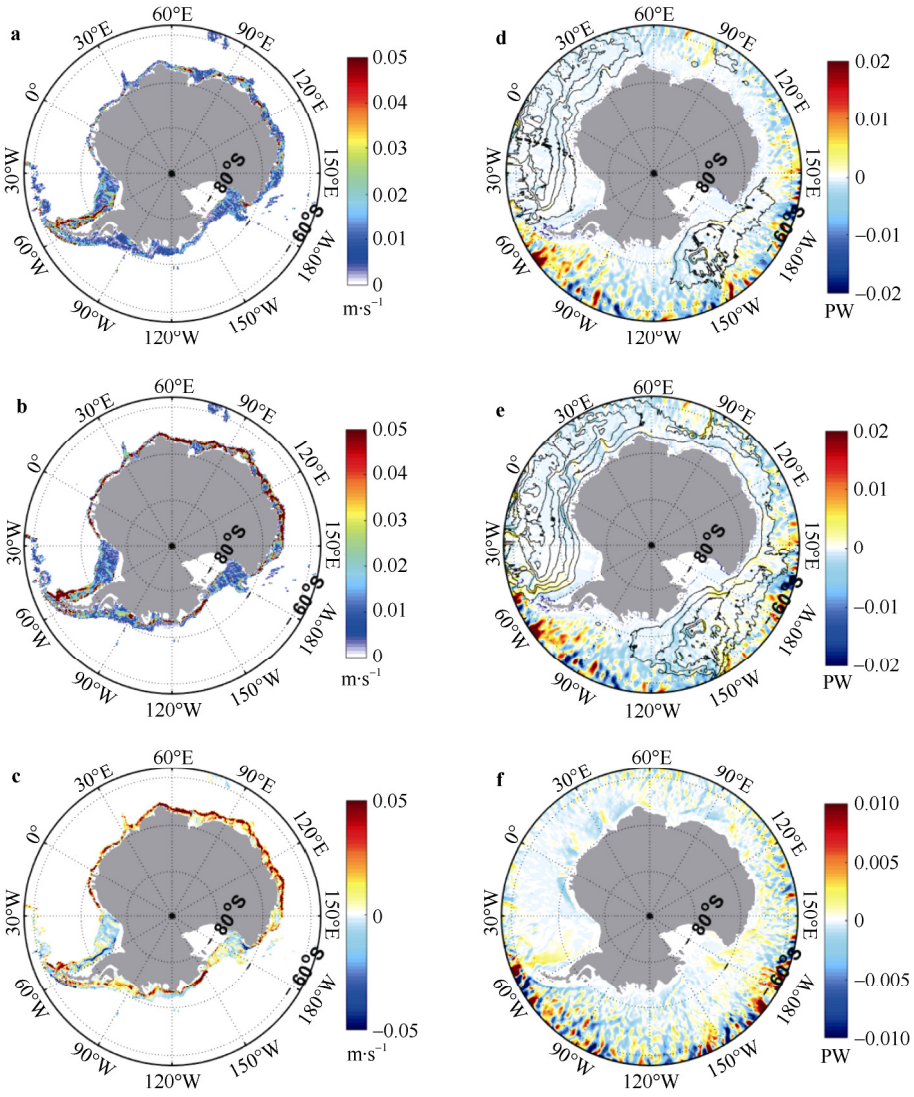

Figure 3 The mean speed of ASBW (**a**–**c**, $m \cdot s^{-1}$), barotropic streamfunction (**d**, **e**, contour lines, 1 Sv=10^6 $m^3 \cdot s^{-1}$) and meridional heat transport (MHT) of the upper 1007.2 m (**d**–**f**, colors, 1 PW=10^{15} W) under atmospheric forcing in 1992 (**a**, **d**) and 1998 (**b**, **e**). **c** shows **b** minus **a**. **f** shows MHT is equal to **e** minus **d**. The contours for the barotropic streamfunction start from the Antarctic coast at 5 Sv with an interval of 10 Sv.

Table 1 Gyre strengths of the Weddell Gyre (WG), Ross Gyre (RG), and Australia-Antarctic Gyre (AG) under different atmospheric forcing

	a: gyre strengths under 1992 forcing/Sv	b: gyre strengths under 1998 forcing/Sv	(b–a)/Sv
WG	62.86	70.74	7.88
RG	46.04	57.10	11.06
AG	15.28	27.28	12.00

warmer water westward. Wind stress close to and parallel to the Antarctic coastline and the corresponding Ekman transport under different atmospheric forcing are also calculated to investigate the local forcing effects on ASBW temperature. The cooling effects of local forcing can be neglected compared to the warming effects from the oceanic heat transport (not shown). Both increased poleward heat transport and ASBW speed contribute to the intense warming of ASBW under strong SH westerlies in 1998.

4 Discussion

The SH westerlies have been strengthening and shifting poleward since the 1970s. However, the impact of recent SH westerly variability on the temperature changes around Antarctica is not clear. This study investigated the response of ASBW temperature to the strengthened SH westerlies. In our model results, the ASBW under the atmospheric forcing with strong SH westerlies in 1998 is warmer in most regions around Antarctica, except the region from 60.125°W to 150.125°W, than that under the atmospheric

forcing with weak SH westerlies in 1992. This is consistent with the observational results obtained by Schmidtko et al. (2014). They showed increased ASBW temperature in the Weddell Sea, Ross Sea and Amundsen Sea, with decreased ASBW temperature in the Bellingshausen Sea in 1998 compared with the results in 1992. The main reasons for the warming of ASBW in most regions around Antarctica are the shoaling and warming of CDW accompanied with strengthened subpolar gyres. The intense shoaling and warming of CDW is due to increased Ekman pumping under stronger SH wind stress curl. Also, strengthened gyres transport more warm water to the coast of Antarctica, contributing to the warming of ASBW. In the future runs of CMIP3 and CMIP5 models, overall strengths of gyres are intensified under strengthened SH westerlies, particularly in the CMIP5 models (Wang, 2013), which is consistent with the results of our simulation. The cooling of ASBW among the coast of the western Antarctic Peninsula is caused by the stronger coastal currents, which transport colder water from the northwest sector of Weddell Sea to the coast of the western Antarctic Peninsula.

Warm ocean water that circulates below the ice shelves leads to basal melting and can cause the instability of ice shelves and the ice sheet (Schoof, 2007). The melting rates near the grounding lines of ice shelves have a strong positive correlation with ocean thermal forcing (Rignot and Jacobs, 2002). The intrusion of CDW onto the continental shelf delivers heat to the base of ice shelves (Jacobs S et al., 2012; Jacobs S S et al., 2011), which enhances the sensitivity of ice-shelf melting to water temperatures at intermediate depth in the Amundsen Sea (Dutrieux et al., 2014; Heimbach and Losch, 2012). Stronger SH westerlies can lead to more CDW intrusion around East Antarctica, which has potential influences on the future stability of ice shelves around East Antarctica (Hellmer et al., 2012).

Our model results indicate that the heat transported by subpolar and Antarctic continental shelf circulations is crucial for ASBW temperature variability. Studies using idealized ocean models, with finer resolution, show that mesoscale eddies and tides can also affect the heat transport and stratification around the Antarctic slope front (Flexas et al., 2015; Stewart and Thompson, 2013; Nøst et al., 2011). In order to get more accurate simulations of the Antarctic coastal environment in the future, the horizontal resolution of the models needs to be increased to higher than 1/50° to resolve the first baroclinic deformation radius (Hallberg, 2013). Iceberg calving and basal melting of ice shelves, which are not included in our model, can also affect the temperature and salinity of ASBW (Rye et al., 2014; Hellmer, 2004). Results derived from a high-resolution regional ocean-sea ice-ice shelf model of the west Antarctic Peninsula indicate that strengthening westerlies, CDW intrusion and ice shelf basal melt rate play important roles in modulating ASBW temperature (Dinniman et al., 2012). To better understand the variability in ASBW temperature, the influences of mesoscale eddies, tides, iceberg calving and basal melting of ice shelf on the Antarctic coastal ocean environment need to also be investigated in the future.

Acknowledgments This study is supported by the National Key R&D Program of China (Grant no. 2016YFA0601804). ZW is supported by the Fundamental Research Funds for the Central Universities (Grant nos. 2017B04814, 2017B20714).

References

Adcroft A, Campin J M, Hill C, et al. 2004. Implementation of an atmosphere ocean general circulation model on the expanded spherical cube. Mon Wea Rev, 132(12): 2845-2863.

Dinniman M S, Klinck J M, Hofmann E E. 2012. Sensitivity of Circumpolar Deep Water transport and ice shelf basal melt along the West Antarctic Peninsula to changes in the winds. J Climate, 25(14): 4799-4816.

Dutrieux P, De Rydt J, Jenkins A, et al. 2014. Strong sensitivity of Pine Island ice-shelf melting to climatic variability. Science, 343(6167): 174-178.

Flexas M D M, Schodlok M P, Padman L, et al. 2015. Role of tides on the formation of the Antarctic Slope Front at the Weddell-Scotia Confluence. J Geophys Res, 120(5): 3658-3680.

Fogwill C J, Turney C S, Meissner K J, et al. 2014. Testing the sensitivity of the East Antarctic Ice Sheet to Southern Ocean dynamics: Past changes and future implications. J Quat Sci, 29(1): 91-98.

Gill A E. 1973. Circulation and bottom water production in the Weddell Sea. Deep Sea Res Oceanogr Abstr, 20(2): 111-140.

Gouretski V. 1999. The large-scale thermohaline circulation of the Ross Sea//Spezie G, Manzella G M R. Oceanography of the Ross Sea, Antarctica. Milan: Springer, 77-100.

Hallberg R. 2013. Using a resolution function to regulate parameterizations of oceanic mesoscale eddy effects. Ocean Modelling, 72: 92-103.

Heimbach P, Losch M. 2012. Adjoint sensitivities of sub-ice-shelf melt rates to ocean circulation under the Pine Island Ice Shelf, West Antarctica. Ann Glaciol, 53(60): 59-69.

Hellmer H H. 2004. Impact of Antarctic ice shelf basal melting on sea ice and deep ocean properties. Geophys Res Lett, 31(10): L10307.

Hellmer H H, Kauker F, Timmermann R, et al. 2012. Twenty-first-century warming of a large Antarctic ice-shelf cavity by a redirected coastal current. Nature, 485(7397): 225-228.

Jacobs S, Jenkins A, Hellmer H, et al. 2012. The Amundsen sea and the Antarctic ice sheet. Oceanography, 25(3): 154-163.

Jacobs S S, Jenkins A, Giulivi C F, et al. 2011. Stronger ocean circulation and increased melting under Pine Island Glacier ice shelf. Nature Geosci, 4(8): 519-523.

Jenkins A, Jacobs S. 2008. Circulation and melting beneath George VI ice shelf, Antarctica. J Geophys Res-Oceans, 113, C04013, doi: 10.1029/2007JC004449.

Klatt O, Fahrbach E, Hoppema M, et al. 2005. The transport of the Weddell Gyre across the prime meridian. Deep-Sea Res Pt II, 52(3-4): 513-528.

Liu C, Wang Z, Cheng C, et al. 2017. Modeling modified Circumpolar Deep Water intrusions onto the Prydz Bay continental shelf, East Antarctica. J Geophys Res-Oceans, 122(7): 5198-5217.

Losch M, Menemenlis D, Campin J M, et al. 2010. On the formulation of sea-ice models. Part 1: Effects of different solver implementations and parameterizations. Ocean Modelling, 33(1-2): 129-144.

Marshall J, Adcroft A, Hill C, et al. 1997a. A finite-volume, incompressible Navier Stokes model for studies of the ocean on parallel computers. J Geophys Res, 102(C3): 5753-5766.

Marshall J, Hill C, Perelman L, et al. 1997b. Hydrostatic, quasihydrostatic, and nonhydrostatic ocean modeling. J Geophys Res-Oceans, 102(C3): 5733-5752.

Marshall G J. 2003. Trends in the Southern Annual Mode from observations and reanalysis. J Climate, 16(24): 4134-4143.

McCartney M S, Donohue K A. 2007. A deep cyclonic gyre in the Australian-Antarctic basin. Progr Oceanogr, 75(4): 675-750.

Menemenlis D, Campin J M, Heimbach P, et al. 2008. ECCO2: High resolution global ocean and sea ice data synthesis. Mercator Ocean Q Newsl, 31: 13-21.

Menemenlis D, Fukumori I, Lee T. 2005. Using Green's functions to calibrate an ocean general circulation model. Mon Weather Rev, 133(5): 1224-1240.

Nøst O A, Biuw M, Tverberg V, et al. 2011. Eddy overturning of the Antarctic Slope Front controls glacial melting in the Eastern Weddell Sea. J Geophys Res-Oceans, 116(C11): C11014.

Oke P R, England M H. 2004. Oceanic response to changes in the latitude of the Southern Hemisphere subpolar westerly winds. J Climate, 17(5): 1040-1054.

Onogi K, Tsutsui J, Koide H, et al. 2007. The JRA-25 Reanalysis. J Meteorol Soc JPN, 85(3): 369-432.

Park Y H, Gambéroni L. 1995. Large-scale circulation and its variability in the south Indian Ocean from TOPEX/POSEIDON altimetry. J Geophys Res-Oceans, 100(C12): 24911-24929.

Rignot E, Jacobs S S. 2002. Rapid bottom melting widespread near Antarctic ice sheet grounding lines. Science, 296(5575): 2020-2023.

Rind D. 1998. Latitudinal temperature gradients and climate change. J Geophys Res-Atoms,103(D6): 5943-5971.

Rye C D, Garabato A C N, Holland P R. 2014. Rapid sea-level rise along the Antarctic margins in response to increased glacial discharge. Nature Geosci, 7(10): 732.

Schmidtko S, Heywood K J, Thompson A F, et al. 2014. Multidecadal warming of Antarctic waters. Science, 346(6214): 1227-1231.

Schoof C. 2007. Ice sheet grounding line dynamics: Steady states, stability, and hysteresis. J Geophys Res-Earth, 112(F3): F03S28.

Spence P, Griffies S M, England M H, et al. 2014. Rapid subsurface warming and circulation changes of Antarctic coastal waters by poleward shifting winds. Geophys Res Lett, 41(13): 4601-4610.

Stewart A L, Thompson A F. 2013. Connecting Antarctic cross-slope exchange with Southern Ocean overturning. J Phys Oceanogr, 43(7): 1453-1471.

Thompson D W J, Solomon S. 2002. Interpretation of recent Southern Hemisphere climate change. Science, 296(5569): 895-899.

Thompson D W J, Solomon S, Kushner P J, et al. 2011. Signatures of the Antarctic ozone hole in Southern Hemisphere surface climate change. Nature Geosci, 4(11): 741.

Wang Z. 2013. On the response of Southern Hemisphere subpolar gyres to climate change in coupled climate models. J Geophys Res-Oceans, 118(3): 1070-1086.

Wang Z, Kuhlbrodt T, Meredith M P. 2011. On the response of the Antarctic Circumpolar Current transport to climate change in coupled climate models. J Geophys Res-Oceans, 116(C8): C08011.

Wang Z, Meredith M P. 2008. Density-driven Southern Hemisphere subpolar gyres in coupled climate models. Geophys Res Lett, 35(14): L14608

Webber B G M, Heywood K J, Stevens D P, et al. 2017. Mechanisms driving variability in the ocean forcing of Pine Island Glacier. Nature Commun, 8: 14507.